CHEMISTRY
A EUROPEAN JOURNAL

DOI: 10.1002/chem.200800825

BINOL-3,3′-Triflone *N*,*N*-Dimethyl Phosphoramidites: Through-Space $^{19}F,^{31}P$ Spin–Spin Coupling with a Remarkable Dependency on Temperature and Solvent Internal Pressure

Matthias Kruck,[a] M. Paz Munoz,[a] Hannah L. Bishop,[a] Christopher G. Frost,[b] Christopher J. Chapman,[b] Gabriele Kociok-Köhn,[b] Craig P. Butts,*[a] and Guy C. Lloyd-Jones*[a]

Abstract: A combined computational and experimental study of the effects of solvent, temperature and stereochemistry on the magnitude of the through-space spin–spin coupling between ^{31}P and ^{19}F nuclei which are six-bonds apart is described. The reaction of 3-trifluoromethylsulfonyl-2,′2-dihydroxy-1,1′-binaphthalene (3-SO_2CF_3-BINOL) with hexamethylphosphorous triamide ($P(NMe_2)_3$) generates a pair of *N*,*N*-dimethylphosphoramidites which are diastereomeric due to their differing relative configurations at the stereogenic phosphorous centre and the axially chiral (atropisomeric) BINOL unit. Through-space NMR coupling of the ^{31}P and ^{19}F nuclei of the phosphoramidite and sulfone is detected in one diastereomer only. In the analogous *N*,*N*-dimethylphosphoramidite generated from 3,3′-$(SO_2CF_3)_2$-BINOL only one of the diastereotopic trifluoromethylsulfone moieties couples with the ^{31}P of the phosphoramidite. In both cases, the magnitude of the coupling is strongly modulated (up to 400%) by solvent and temperature. A detailed DFT analysis of the response of the coupling to the orientation of the CF_3 moiety with respect to the P-lone pair facilitates a confident assignment of the stereochemical identity of the pair of diastereomers. The analysis shows that the intriguing effects of environment on the magnitude of the coupling can be rationalised by a complex interplay of solvent internal pressure, molecular volume and thermal access to a wider conformational space. These phenomena suggest the possibility for the design of sensitive molecular probes for local environment that can be addressed via through-space NMR coupling.

Keywords: conformation analysis · coupling · NMR spectroscopy · solvent effects · stereochemistry

Introduction

Phosphoramidites derived from 2,2′-dihydroxy-1,1′-binaphthalene (BINOL, **1**) were first reported by Feringa[1] in 1994 and have been developed as extremely effective monodentate ligands for a wide range of asymmetric catalytic processes.[2] In a number of cases, symmetrical 3,3′-bis-substitution of the binaphthalene skeleton has been shown to be crucial for the asymmetric induction,[3] and significant effort has been made to develop syntheses for these compounds.[4] We recently reported the preparation of enantiomerically pure bis-3,3′-SO_2R^F-substituted BINOLs,[5] by way of an anionic thia-Fries rearrangement[6] of bis O-SO_2R^F esters of BINOL **1**, and their highly effective application as catalysts for the asymmetric indium mediated allylation of hydrazones.[5] Using the standard procedure for phosphoramidite generation,[1] this rearrangement now provides rapid access

[a] M. Kruck, Dr. M. P. Munoz, H. L. Bishop, Dr. C. P. Butts, Prof. G. C. Lloyd-Jones
School of Chemistry, University of Bristol, Cantock's Close
Bristol, BS81TS (UK)
Fax: (+44) 117-929-8611
E-mail: Craig.Butts@bris.ac.uk
Guy.Lloyd-Jones@bris.ac.uk

[b] Dr. C. G. Frost, Dr. C. J. Chapman, Dr. G. Kociok-Köhn
Department of Chemistry, University of Bath
Claverton Down, Bath, BA72AY (UK)

Supporting information for this article is available on the WWW under http://dx.doi.org/10.1002/chem.200800825: Full experimental details for the synthesis and characterisation of **2** and **3**, details of computations and full datasets of solvent and temperature dependencies of J_{PF}.

to new monodentate ligands of type **2**, in just three steps from **1**[7] (Scheme 1).

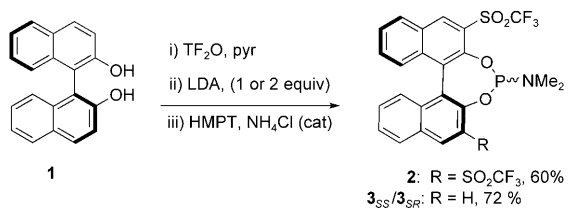

Scheme 1. Synthesis of triflone-BINOL phosphoramidites (*S*)-**2** and $\mathbf{3}_{SR}$/$\mathbf{3}_{SS}$ (66:34 to 83:17 *dr*); yields correspond to step iii).

A key feature of the rearrangement[5,6] is that by use of just one equiv LDA, it provides mono-substituted 3-SO_2R^F-BINOLS and thus phosphoramidite ligands of type **3**. However, the introduction of only one substituent onto the BINOL backbone reduces the symmetry from C_2 to C_1 resulting in a stereogenic centre at the phosphorous and thus two diastereomeric forms ($\mathbf{3}_{SR}$ and $\mathbf{3}_{SS}$). Reetz[8] has elegantly demonstrated that this type of desymmetrisation can give rise to interesting effects in catalysis using BINOL phosphoramidites. For example, significant match–mismatch effects can be found by use of partially or fully resolved diastereomers,[8] and remarkably, the enantioselectivity can even be reversed as compared to C_2-symmetric systems.

Although bis-triflone (*S*)-**2** recrystallised readily (see X-ray structure in Figure 1), we were unable to obtain suitable crystals of either diastereoisomer of monotriflone **3**[9] so as to assign their identities.[10] However, we did find that **2** and one diastereoisomer of **3** gave rise to unexpectedly information-rich ^{19}F and ^{31}P NMR spectra, displaying "through-space" coupling between phosphorous and fluorine nuclei. "Through-space" scalar coupling between NMR active nuclei was first reported in the 1950s[11] and a number of studies have identified that it is transmitted through an antibonding interaction between the lone pairs of the two nuclei.[12] It is known that the magnitude of the coupling decays rapidly as the distance exceeds the sum of the van der Waals radii of the coupled nuclei,[13] however, the behaviour of this coupling with respect to changes in the molecular environment are much less well documented.

Herein we report on the remarkably solvent and temperature-dependent "through-space" ^{31}P–^{19}F coupling in **2** and **3**. A detailed computational analysis of the conformational and distance dependency of this phenomenon has allowed a confident stereochemical assignment of $\mathbf{3}_{SR}$/$\mathbf{3}_{SS}$ and illustrates the potential for design of new NMR-addressable molecular probes.

Results and Discussion

The $^{19}F\{^1H\}$ NMR spectra of the two diastereomers **3** in $CDCl_3$ shows the expected CF_3 signals at δ −76.33 and −76.14 ppm, respectively, however, in the latter case the ^{19}F resonance exhibits as a doublet (J = 5.2 Hz). In the corresponding $^{31}P\{^1H\}$ NMR spectra of **3**, signals at δ 151.3 and 155.5 ppm were observed as a singlet and a quartet (J = 5.2 Hz) respectively, confirming that in one diastereoisomer only the three equivalent ^{19}F nuclei of the triflone, time-averaged by rotation around the S–CF_3 bond, couple to the ^{31}P nucleus. Such a coupling, which relies on near VDW contact between the lone pairs, is certainly remarkable given the six-bond internuclear separation and relative conformational freedom within the structure, in particular that of the triflone group (Figure 2).

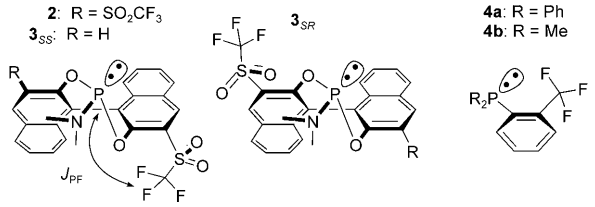

Figure 2. Schematic representation of the disposition of the P-based lone pair and the triflone group(s) in **2** and **3**, based on the X-ray structure of **2**. Also shown are phosphanes **4a** and **4b** which display relatively temperature insensitive through-space P–F coupling, due to dominance of the through-bond scalar coupling $^4J_{PF}$.

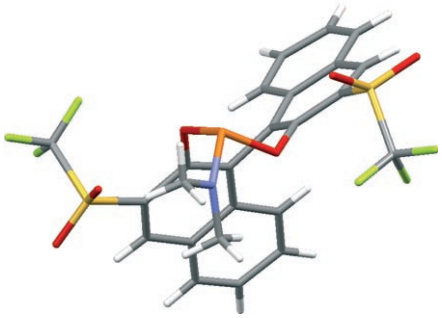

Figure 1. Single-crystal X-ray structure of (*S*)-**2**; C (grey); H (white); N (blue); O (red); F (green); S (yellow); P (orange). The asymmetrical unit contains 0.5 molecules of water (not shown) that are distributed about two special positions. There are also voids in the structure which suggest that up to three more molecules of water are present.

A similar through-space coupling is observed between the phosphorous and only one of the triflone groups in the bis-triflone **2** ($CDCl_3$, room temperature) giving a doublet (δ −76.16 ppm, J = 5.5 Hz) and singlet (δ −76.25 ppm) in the ^{19}F NMR spectrum, while the ^{31}P NMR spectrum again shows the corresponding quartet (δ 157.2 ppm, J = 5.5 Hz).

The X-ray crystallographic structure of bis-triflone **2** (Figure 1) shows that both triflone CF_3 groups occupy positions roughly perpendicular to the pyramidalised ^{31}P lone pair (Figure 2), and provides no clear evidence as to which CF_3 is coupled to the phosphorous. The phosphorous lone pair is clearly oriented towards one of the naphthyl rings (and thus one triflone group), hence one might assume that this is the triflone CF_3 which couples—thus allowing an assignment of $\mathbf{3}_{SR}$ and $\mathbf{3}_{SS}$. However, recent analyses of orbital

contributions to through-space coupling[13] suggest that orbital contributions to through-space coupling can be significantly more complex than is first apparent. One obvious alternative is that the coupling could arise by overlap of the ^{19}F lone pairs with the back lobe of the phosphorous lone-pair, which would give rise to the opposite structural assignments for $\mathbf{3}_{SR}$ and $\mathbf{3}_{SS}$.

Structural assignment of the diastereomers of 3: To further explore the distinct difference in ^{31}P and ^{19}F NMR spectra exhibited by the two diastereomers of **3** ($\mathbf{3}_{SR}$ and $\mathbf{3}_{SS}$), the configurational dependence of the through-space ^{31}P,^{19}F coupling constants were calculated using density functional theory with a $Me_2NP(OH)_2$–CF_4 pair. The CF_4 molecule was positioned across a range of P–C separations (r_{PC}) and (lonepair)-P-C angles (θ), and the CF_3 rotation averaged J_{PF} was calculated for each. A summary of results are presented in Figure 3 and shows that only a small window of geometries (r_{PC} = 5.7–6.1 Å, θ = 0–55°) can give rise to calculated

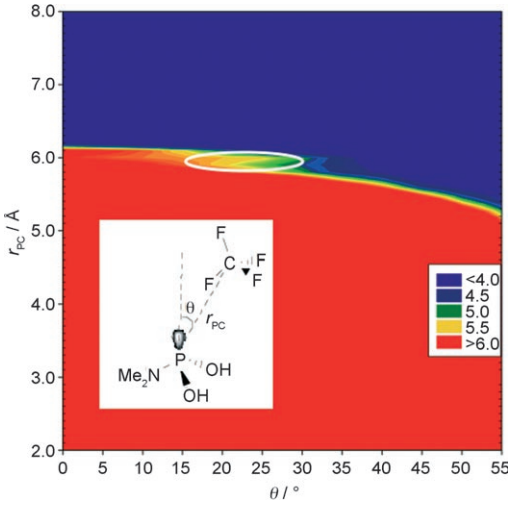

Figure 3. Contour plot of calculated J_{PF} using a $Me_2NP(OH)_2$–CF_4 pair with a range of geometries defined by their separation (r_{PC}, y axis) and lone pair-P-C angle (θ, x axis). Geometries compatible with J_{PF} values observed for **2** and one diastereomer of **3** ($\mathbf{3}_{SS}$) are highlighted within the white ellipsoid.

J_{PF} values which are of comparable magnitude to the experimental J_{PF} values for **2** and **3** (4–6 Hz). Moreover, within these, only a very narrow range ($35 > \theta > 10°$, circled) correlate well. In other words, the only acceptable CF_3 locations for the observed J_{PF} values are concentrated in the region of, and slightly off axis from, the main lobe of the ^{31}P lone pair.

Geometries with $\theta > 55°$ are discounted on the basis that they involve a clash between the CF_3 and the phosphorous substituents. It is also notable that the calculated magnitude of the coupling is insignificant from the back face of the phosphorous ($\theta > 125°$) except at significantly reduced distances ($r_{PC} \ll 5.0$ Å) which can again be discounted on consideration of the steric constraints. On this basis, the structure of the diastereoisomer that shows the ^{31}P–^{19}F coupling is assigned to $\mathbf{3}_{SS}$ (Figure 2).

The effect of solvent internal pressure (P_i) on J_{PF}: The response of the coupling constant to changes in environment also provides structural insight. It was found that changes in the NMR solvent also induce a significant variation in the measured J_{PF} at all temperatures, for example, 4.0 and 5.5 Hz for **2** in toluene and $CDCl_3$, respectively, at room temperature. A range of deuterated and non-deuterated solvents were investigated and although a variety of J_{PF} values for **2** were observed, there was no trend with common solvent parameters, for example, dielectric constant (ξ) (see Supporting Information), indeed measurements in polar protic solvents give low coupling constants (CH_3OH 3.90 Hz, *i*PrOH 4.19 Hz) of comparable magnitude to those measured in non-polar solvents (hexane 4.20 Hz, toluene 3.98 Hz), while polar aprotic solvents give rise to relatively high coupling constants (DMSO 5.60 Hz, DMF 4.99 Hz) at room temperature. Attempts to correlate this behaviour in multicomponent fits were also unsuccessful. In the event only one parameter, solvent internal pressure (P_i),[14,15] was found to show any significant correlation with the observed coupling constant in the range of solvents examined (Figure 4). While the fit is clearly imperfect ($R^2 = 0.59$), the majority of data in Figure 4 fall within ±0.4 Hz of the predicted (trend-averaged) value based on their internal pressure, with the only significant deviations from the trend being chloroform ($J = 5.50$ Hz, $P_i = 369$ MPa) and toluene ($J = 3.98$ Hz, $P_i = 354$ MPa).[16]

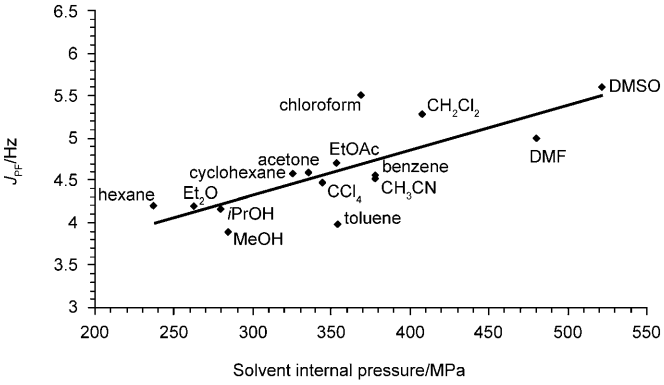

Figure 4. Correlation of the observed J_{PF} (y axis) for **2** in a variety of solvents with solvent internal pressure (P_i, x axis).[14,15]

It should be noted that independent literature values for solvent internal pressure, P_i,[14,15] are limited with the majority arising indirectly from citation to a single source.[15] Interestingly, the related solvent parameter, cohesive pressure, c, does not show any correlation with the observed J_{PF}, suggesting that specific solvent interactions such as hydrogen-bond donation have little or no part to play in the observed behaviour, this being consistent with, for example, the near-identical couplings found in *i*PrOH versus hexane. Solvent internal pressure, P_i,[14,15] can be considered a measure of the pressure imposed on a solute molecule by the surrounding solvent.[14] Thus the observed solvent dependence of J_{PF} can be interpreted as a response to a change in the average molecular volume of **2** in the various solvents. In general

terms, this interpretation would suggest that an increased solvent pressure encourages **2** to favour conformations with lower molecular volumes, hence causing the time-averaged distance between the phosphorous and fluorine nuclei to be slightly reduced and hence a larger J_{PF} under higher solvent internal pressure. In both **2** and $\mathbf{3}_{SS}$, such a reduction in molecular volume could arise from a combination of two conformational phenomena: i) rotation around the aryl–S bond to bring the larger CF_3 group *syn* to the binaphthyl C2–C3 bond, and ii) narrowing of the binaphthyl "pincer" angle. Close consideration of these two phenomena suggests that while aryl–S bond rotation will indeed bring the CF_3 closer to the phosphorous nuclei, thus giving rise to an increase in J_{PF}, changes in pincer angle would serve to flatten the binaphthyl moiety, resulting actually in an increase in angle θ (Figure 3) and hence reducing J_{PF} (see below). Given the relative freedom of rotation of the triflone group about the aryl–S bond, contrasted with the high energetic costs of binaphthyl pincer deformation, it is not surprising that aryl–S rotation dominates ΔJ_{PF}. DFT calculations of the molar volume of $\mathbf{3}_{SS}$ support this suggestion as the gas-phase geometry-optimised structure (C2-C3-S-CF_3 dihedral angle of 64°) occupies ≈5% more volume than the alternative structure where the S–CF_3 bond is *syn* to the C2–C3 bond, that is, with the CF_3 oriented directly towards the phosphoramidite substituent (329 and 308 cm^{-3} per mol, respectively), hence the CF_3 will prefer to occupy the space closer to the phosphorus under higher solvent pressures.

The effect of temperature on J_{PF}: In addition to the effect of solvent a substantial effect of temperature on J_{PF} was also apparent. Spectra in chloroform, toluene and acetone across a range of temperatures (−58 to +100 °C) showed that the magnitude of J_{PF} in **2** and $\mathbf{3}_{SS}$ exhibit substantial and positive temperature dependencies (Figure 5). Notably, J_{PF} for $\mathbf{3}_{SS}$ in [D_8]toluene increased nearly four-fold from 1.66 to 6.50 Hz between −40 and +100 °C. Both **2** and $\mathbf{3}_{SS}$ show similar, approximately linear, dependence of J_{PF} against either T or $1/T$, with comparable temperature coefficients (ΔJ_{PF} ≈3.25 ± 0.25 Hz at 100 °C) in all of the solvents tested. The effect of temperature on through-space ^{31}P–^{19}F coupling constants in diphenylphosphine **4a** (Figure 2) was previously noted by Miller et al.[16] (Table 1, ΔJ_{PF} ≈2 Hz at 100 °C). In contrast to **2** and $\mathbf{3}_{SS}$ where the magnitude of $^6J_{PF}$ is negligible, the coupling observed in **4a** predominantly arises from a large 4-bond scalar coupling ($J_{PF}(obsd) = {}^4J_{PF} + J_{PF}$) and thus only a ≈5% change is observed across 132 °C, as compared to ≈400% in **2**. Miller et al. ascribed the temperature dependence of J_{PF} in **4a** to increased amplitudes of torsional oscillations around the aryl–CF_3 bond, away from the lowest energy conformation.

To examine the effect of temperature on J_{PF}, rotation of the CF_3 group in **4a** was modelled using the closely related dimethylphosphino analogue **4b** and the rotation-averaged J_{PF} at each temperature was established by calculating both J_{PF} and the absolute (gas-phase) energies of CF_3 rigid rotamers of **4b**. The angle between the plane of the aryl ring and each C–F bond was incremented in 10° steps and a Boltzmann population distribution assumed at each temperature. The results are summarised in Table 1 and confirm that the change in J_{PF} for **4b** (ΔJ_{PF} ≈3 Hz at 100 °C) can be entirely accounted for on the basis of the temperature dependence of the Boltzmann populations of the contributing rotamers.

Table 1. Comparison of the temperature dependence of J_{PF} in 1-diphenylphosphino-2-trifluoromethylbenzene (**4a**) reported by Miller et al.[16] with that calculated for model compound 1-dimethylphosphino-2-trifluoromethylbenzene (**4b**).

Entry	T/K	J_{PF} obsd[a] **4a**	ΔJ^{258}[b]/%	J_{PF} calcd[c] **4b**	ΔJ^{258}[b]/%
1	258	54.23	0.0	59.15	0.0
2	298	55.00	1.4	60.06	1.5
3	348	55.98	3.2	61.69	4.3
4	390	56.73	4.6	62.86	6.3

[a] values taken from reference [16]; [b] the percent change in the coupling constant from that observed (**4a**) or predicted (**4b**) at 258 K; [c] based on the net J_{PF} calculated by DFT using a Boltzmann-weighted ensemble of populations of Ar–CF_3 rotamers. See text and Supporting Information for full details.

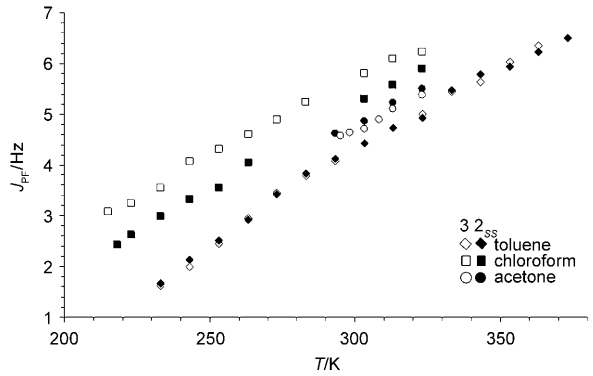

Figure 5. Effect of temperature (T/K, x axis) on the magnitude of the through-space coupling constant (J_{PF}/Hz, y axis) in phosphoramidites **2** and $\mathbf{3}_{SS}$ in toluene, chloroform and acetone.

In the case of phosphoramidites **2** and $\mathbf{3}_{SS}$, the temperature effect (ΔJ_{PF} ≈3.25 Hz at 100 °C) likely arises from a more complex expression of this same effect, namely increased displacement around the biaryl- and aryl–S bonds, leading to greater populations of conformations with both smaller and greater average ^{31}P–^{19}F lone pair separations. As the magnitude of through-space coupling has a strong, inverse non-linear dependence on r_{PF}, those conformations with smaller r_{PF} dominate J_{PF} and thus the increased thermal motion leads to a time-averaged increase in the observed coupling constant. By analogy with the arguments made above regarding solvent effects, it is likely that the aryl–S bond rotation is the key conformational feature controlling the observed temperature dependence. It should also be noted that the temperature dependence of solvent internal pressure P_i,[14,15] can be excluded as a contributing factor since it is of significantly lower magnitude (ΔP_i is typically 0 to +10 Pa K^{-1}, that is, <0.01% K^{-1}) than the observed temperature dependence of J_{PF}.[17]

Conclusion

In summary, the through-space coupling observed by NMR between ^{31}P and ^{19}F nuclei in flexible triflone-bearing phosphoramidite ligands have been analysed by computation, allowing a confident stereochemical assignment of the diastereoisomers **3**. Furthermore, there is a marked dependence of J_{PF} on increasing solvent internal pressure, P_i,[14,15] ascribed to changes in the conformational population distribution to adopt structures with lower molecular volumes. Similarly, the positive temperature dependence of J_{PF} in both **2** and $\mathbf{3}_{SS}$ (ca. 3.25 ± 0.25 Hz at 100 °C) is assigned to increased population of high-energy conformers at higher temperatures, with conformations possessing small P–F separations dominating the contributions to ΔJ_{PF}. On the basis of the substantial modulation of J_{PF} observed in **2** and $\mathbf{3}_{SS}$, we are currently exploring the design and synthesis of new molecules in which we can exploit such through-space NMR coupling as a probe for molecular responses to changes in local environment.

Experimental Section

Spectroscopic determination of J_{PF}: NMR spectra were measured on a JEOL ECP300 spectrometer. ^{19}F and ^{31}P FIDs were acquired with 65536 data points. Data processing was undertaken using Delta or ACDLabs software and the FIDs were zero-filled to 524288 points and resolution enhanced with a Lorentzian-Gaussian window function (LB = −1.5, GF = 0.35) prior to Fourier transform. Coupling constants were measured manually from the spectrum. Absolute temperatures of NMR samples are uncalibrated and errors of relative temperature for a given experiment are ±0.5 °C. Geometry optimisations and computation of coupling constants were undertaken using the Gaussian03 or Gaussian03W software. Calculations employed density functional theory using the B3LYP functional, with both geometries and NMR parameters calculated with a 6-311** basis set for all atoms. Molar volume calculations were conducted using the same method and basis sets as above, with the "Volume = Tight" option in Gaussian03.

CCDC 644613 [(*S*)-**2**)] contains the supplementary crystallographic data for this paper. These data can be obtained free of charge from The Cambridge Crystallographic Data Centre via www.ccdc.cam.ac.uk/data_request/cif.

Acknowledgement

We thank the European Union (STRP 505167-1 LIGBANK) for support and the MEC (Spain) for a Fellowship (M.P.M.).

[1] R. Hulst, N. K. de Vries, B. L. Feringa, *Tetrahedron: Asymmetry* **1994**, *5*, 699–708.

[2] Representative examples: a) conjugated addition of alkylzinc reagents to ketones: B. L. Feringa, *Acc. Chem. Res.* **2000**, *33*, 346–353; b) Rh-catalysed asymmetric hydrogenation: H. Bernsman, M. van der Berg, R. Hoen, A. J. Minnaard, G. Mehler, M. T. Reetz, J. G. de Vries, B. L. Feringa, *J. Org. Chem.* **2005**, *70*, 943–951; c) Ni-catalysed hydrovinylation: G. Francio, F. Faraone, W. Leitner, *J. Am. Chem. Soc.* **2002**, *124*, 736–737; d) Ir-catalysed allylic amination: A Leitner, S. Shekhar, M. J. Pouy, J. F. Hartwig, *J. Am. Chem. Soc.* **2005**, *127*, 15506–15514; e) Rh-catalysed arylation of aldehydes: R. B. C. Jagt, P. Y. Toullec, J. G. de Vries, B. L. Feringa, A. J. Minnaard, *Org. Biomol. Chem.* **2006**, *4*, 773–775.

[3] a) D. J. Cram, J. D. Y. Sogah, *Chem. Commun.* **1981**, 625–628; b) K. Narasaka, *Synthesis* **1991**, 1–11; c) A. K. H. Knöbel, I. H. Escher, A. Pfaltz, *Synlett* **1997**, 1429–1431; d) K. Ishihara, H. Yamamoto, *J. Am. Chem. Soc.* **1994**, *116*, 1561–1562.

[4] a) D. J. Cram, R. C. Helgeson, S. C. Peacock, L. J. Kaplan, L. A. Domeier, P. Moreau, K. Koga, J. M. Mayer, Y. Chao, M. G. Siegel, D. H. Hoffman, G. D. Sogah, *J. Org. Chem.* **1978**, *43*, 1930–1946; b) D. S. Lingenfelter, R. C. Helgeson, D. J. Cram, *J. Org. Chem.* **1981**, *46*, 393–406; c) P. J. Cox, W. Wang, V. Snieckus, *Tetrahedron Lett.* **1992**, *33*, 2253–2256; d) L. A. Arnold, R. Imbos, A. Mandoli, A. H. M. de Vries, R. Naasz, B. L. Feringa, *Tetrahedron* **2000**, *56*, 2865–2878.

[5] R. Kargbo, Y. Takahashi, S. Bhor, G. R. Cook, G. C. Lloyd-Jones, I. R. Shepperson, *J. Am. Chem. Soc.* **2007**, *129*, 3846–3847.

[6] a) J. P. H. Charmant, A. M. Dyke, G. C. Lloyd-Jones, *Chem. Commun.* **2003**, 380–381; b) Z. Zhao, J. Messinger, U. Schön, R. Wartchow, H. Butenschön, *Chem. Commun.* **2006**, 3007–3009; c) A. M. Dyke, D. M. Gill, J. N. Harvey, A. J. Hester, G. C. Lloyd-Jones, M. P. Muñoz, I. R. Shepperson, *Angew. Chem.* **2008**, *120*, 5145; *Angew. Chem. Int. Ed.* **2008**, *47*, 5067–5070.

[7] These new ligands, together with their sulfone derivatives ($CF_3 \rightarrow R$), have proven of utility in asymmetric hydrogenation (M. P. Muñoz, I. R. Shepperson, G. C. Lloyd-Jones, W. Leitner, G. Franco, unpublished results).

[8] a) M. T. Reetz, J.-A. Ma, R. Goddard, *Angew. Chem.* **2005**, *117*, 416–419; *Angew. Chem. Int. Ed.* **2005**, *44*, 412–415; b) M. T. Reetz, X. Li, *Angew. Chem.* **2005**, *117*, 3019–3021; *Angew. Chem. Int. Ed.* **2005**, *44*, 2959–2962.

[9] The two diastereomers undergo interconversion at elevated temperatures. A full analysis of the kinetic and thermodynamic aspects of this equilibrium, together with an analogous analysis of the sulfone derivatives ($CF_3 \rightarrow R$), will be reported in full in due course: M. Kruck, M. P. Munoz, C. P. Butts, G. C. Lloyd-Jones, unpublished results.

[10] Reetz has reported (reference [8]) that in species analogous to **3**, where CH_2O_2CPh or $SiPh_3$ replaces SO_2CF_3, the ^{31}P NMR chemical shift order for the diastereomers (assigned by X-ray crystallography) is consistent (δ_P *S*,*S*$_P$ > δ_P *S*,*R*$_P$). This relationship was then employed by Reetz to assign diastereoisomeric identity to a range of other analogues. Whilst the SO_2CF_3 group has rather unique properties,[5,6] the correlation does indeed hold for **3** (δ_P $\mathbf{3}_{SS}$ = 155.50; δ_P $\mathbf{3}_{SR}$ = 151.31).

[11] A. Saika, H. S. Gutowsky, *J. Am. Chem. Soc.* **1956**, *78*, 4818–4819.

[12] For a summary, see: F. B. Mallory, C. W. Mallory, in *Encyclopedia of Nuclear Magnetic Resonance* (Eds.: D. M. Grant, R. K. Harris), Wiley, Chichester, **1996**, pp. 1491.

[13] T. Tuttle, J. Gräfenstein, D. Cremer, *Chem. Phys. Lett.* **2004**, *394*, 5–13.

[14] C. Reichardt, *Solvents and Solvent Effects in Organic Chemistry*, WILEY-VCH, Weinheim, **2003**, pp. 62–66.

[15] G. Allen, G. Gee, G. J. Wilson, *Polymer* **1960**, *1*, 456–466.

[16] G. R. Miller, A. W. Yankowsky, S. O. Grim, *J. Chem. Phys.* **1969**, *51*, 3185–3190.

[17] V. N. Kartsev, M. N. Rodnikova, S. N. Shtykov, *J. Struct. Chem.* **2004**, *45*, 91–95.

Received: May 1, 2008
Published online: July 18, 2008

